Preparation and Magnetoelectric Behavior of Ni/BaTiO$_3$ Heterostructures with 0-3 Connectivity

*Toni Buttlar, Till Walther, Kathrin Dörr, and Stefan G. Ebbinghaus**

Magnetoelectric 0-3 composites consisting of small ferromagnetic Ni particles in the micrometer range embedded in a ferroelectric BaTiO$_3$ matrix are synthesized by reductive sintering in flowing nitrogen with carbon as the oxygen getter. Phase purity of the samples Ni$_x$/(BaTiO$_3$)$_{1-x}$ ($x = 0.1$–0.7) is verified by powder X-ray diffraction in combination with scanning electron microscopy/energy-dispersive X-ray spectroscopy analyses and magnetization investigations. The magnetoelectric coefficient (α_{ME}) is studied for parallel and perpendicular orientations of polarization and magnetic field. For the latter orientation, a reverse sign and a much weaker signal are found. The dependence of α_{ME} on the magnetic direct current bias field shows a linear behavior between $\approx \pm 2$ kOe and a drop to almost zero above ≈ 4 kOe. Largest values are obtained for $x = 0.4$. With increasing frequency of the alternating current driving field, α_{ME} becomes larger. At low temperatures, two step-like decreases in the magnetoelectric coefficient occur, reflecting the phase transitions of BaTiO$_3$ (tetragonal→orthorhombic and orthorhombic→rhombohedral). While this finding corroborates the interpretation of α_{ME} being a product property of magnetostriction and piezoelectricity, distinct deviations between the field dependence of the integrated ME signal and the magnetostriction of nickel are found.

1. Introduction

Materials possessing more than one ferroic-ordering phenomenon are denoted as multiferroics. The mutual interaction of the different orderings opens the door to a variety of new applications. The magnetoelectric effect, i.e., the coupling between

T. Buttlar, Dr. T. Walther, Prof. S. G. Ebbinghaus
Institute of Chemistry
Martin Luther University Halle-Wittenberg
Kurt-Mothes-Strasse 2, 06120 Halle, Germany
E-mail: stefan.ebbinghaus@chemie.uni-halle.de

Prof. K. Dörr
Institute of Physics
Martin Luther University Halle-Wittenberg
Von-Danckelmann-Platz 3, 06120 Halle, Germany

The ORCID identification number(s) for the author(s) of this article can be found under https://doi.org/10.1002/pssb.201900622.

ferro- or ferrimagnetism and ferroelectricity, is one possible coupling effect in multiferroics, which can be classified as single-phase and composite compounds. Prominent examples for single-phase materials are BiFeO$_3$, YMnO$_3$, and HoMnO$_3$. In magnetoelectric composites, one component is ferro- or ferrimagnetic (e.g., CoFe$_2$O$_4$ (CFO) or Tb$_{1-x}$Dy$_x$Fe$_2$ (Terfenol-D)), whereas the second one (like BaTiO$_3$ [BTO] or Pb(ZrTi)O$_3$ [PZT]) shows ferroelectricity, and the coupling is mediated through the interface.[1–6] Such composites can be assembled in different ways. Ferromagnetic particles or fibers enclosed in a ferroelectric matrix are denoted as a 0-3 and 1-3 connectivity, respectively, whereas 2-2 composites consist of alternating layers.[7] A 3-3 connectivity, in which the two phases form a 3D interpenetrating network, can be obtained by eutectic crystallization, e.g., of CFO and BTO.[6,8]

BaTiO$_3$ is a well-investigated material because of its high dielectric permittivity and its various phase transitions. Below $\approx -90\,°C$ (183.15 K), BaTiO$_3$ has a rhombohedral structure; up to $0\,°C$ (273.15 K), it is orthorhombic and between 0 and 120 °C (393.15 K), it is tetragonal. While these three modifications are ferroelectric, the cubic high-temperature phase is paraelectric.[9,10] Magnetoelectric 0-3 composites consisting of BaTiO$_3$ and CoFe$_2$O$_4$ have been widely studied.[4,5,11] In comparison, the combination of BaTiO$_3$ and nickel ($M_S = 0.61\,\mu_B$ (f.u.)$^{-1}$[12] $T_C = 354\,°C$ (627.15 K)[13]) in 0-3 connectivity is far less investigated. One reason might be that it can be difficult to combine these two materials in a magnetoelectric 0-3 composite. Huang et al. showed that there is only a small process window for the generation of dense, highly insulating Ni–BaTiO$_3$ composites because the oxygen partial pressure is a critical factor. If it is too high, nickel is oxidized, whereas a too small value causes oxygen defects in barium titanate, resulting in conducting samples.[14–16]

In this work, we report on the preparation of dense 0-3 Ni–BaTiO$_3$ composites with high resistance in flowing nitrogen with carbon as the oxygen getter. According to an Ellingham diagram[17] based on the data of Barin,[18] carbon reduces the oxygen partial pressure in a nitrogen atmosphere below the level required for the oxidation of nickel. The samples are characterized by X-ray diffraction (XRD), scanning electron microscopy (SEM)/energy-dispersive X-ray spectroscopy (EDX), and
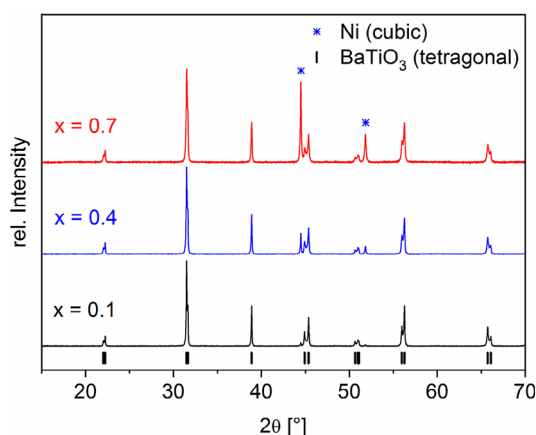
magnetic measurements. Special emphasis is given to the magnetoelectric properties depending external magnetic field and temperature.

2. Results and Discussion

2.1. XRD, SEM, and EDX Results

XRD patterns of selected composites with lowest, medium, and highest Ni content after applying the sintering step at 1623 K (flowing nitrogen with graphite as the oxygen getter) are shown in **Figure 1**. The diffraction patterns after the reduction at 1073 K in forming gas are almost identical and are therefore not shown. In all samples, only Ni metal ($a = 3.524(1)$ Å) and the tetragonal modification of $BaTiO_3$ ($a = 3.995(1)$ Å and $c = 4.030(2)$ Å) were detected. The determined cell parameters did not show any dependence on the Ni content. Therefore, a possible migration of nickel in the $BaTiO_3$ matrix is very unlikely.

The choice of carbon as oxygen getter was based on the Ellingham diagram (shown in **Figure 2**), indicating that pO_2
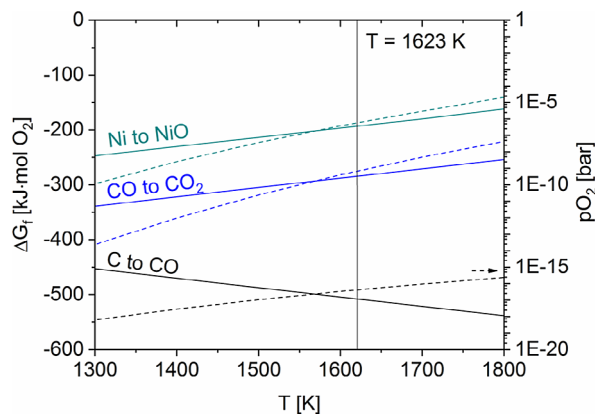
of the system $C/CO/CO_2$ is sufficiently low to avoid the reoxidation of nickel to NiO.[17,18]

Huang et al. described that the process window for the synthesis of dense Ni–$BaTiO_3$ composites with high resistance is rather small with respect to the oxygen partial pressure.[14] At a too high oxygen concentration, nickel oxidizes to NiO, whereas very low oxygen partial pressures lead to electrically conductive barium titanate due to the formation of oxygen defects. Huang et al. achieved best results with an oxygen partial pressure of 10^{-7}–10^{-8} bar, which was measured by a zirconia oxygen sensor positioned above the samples and was adjusted using a mixture of forming gas (N_2/H_2:95/5) and nitrogen. The obtained composites with a nickel content up to 5 vol% ($\approx$25 mol%) exhibited relative densities of over 95%.[14] According to Figure 2, a much lower pO_2 in the range of 10^{-17} bar is expected at 1623 K for C/CO. It has to be noted, though, that Ellingham diagrams only apply for thermodynamic equilibrium, i.e., for closed systems, whereas an open system (nitrogen flow) was used in our case. For our experimental setup, a pO_2 of about $\approx$$10^{-17}$ bar was measured at the furnace outlet, which obviously does not lead to electrically conductive barium titanate.

For our composites, relative densities in the range of 93–96% (see **Table 1**) were derived from the weight and geometric dimensions of the pellets after Marks and Monson,[19] using the crystallographic densities of Ni and $BaTiO_3$. The densities of our composites are very similar to the ones reported in literature, and small deviations of a few percent are not unusual during sintering processes.[14] Attempts to apply higher sintering temperatures led to low resistive composites, which were unsuited for electrical poling, due to the formation of oxygen vacancies.[14]

Figure 3 shows SEM images and equivalent spherical diameter histograms for the Ni particles of three exemplary samples with $x = 0.1$, 0.4, and 0.7. Due to the different Z contrast, nickel and barium titanate appear in dark and light gray, respectively. All samples possess only few and small pores, reflecting their high densities, and consist of basically spherical Ni particles embedded in the $BaTiO_3$ matrix in accordance with the aspired 0-3 connectivity. The sample containing 10 mol% Ni shows well-separated particles with $\approx$0.60 μm diameter. The sample with 40 mol% Ni content still consists of spherical, isolated Ni

Figure 1. XRD pattern of selected Ni_x–$(BaTiO_3)_{1-x}$ composites ($x = 0.1$, 0.4, and 0.7) after sintering in nitrogen at 1623 K for 2 h with carbon as oxygen getter.

Figure 2. Ellingham diagram for the formation of the oxides of nickel and carbon (full lines) and the equilibrium oxygen pressure (dashed lines).

Table 1. Saturation (M_S) and remanent magnetization (M_R), nickel content (nominal and calculated), and relative densities of Ni_x–$(BTO_3)_{1-x}$ composites and of the pure nickel reference.

| Nominal Ni content, x	M_S [emu g (Ni)$^{-1}$] (μ_B f.u.$^{-1}$ Ni)	M_R [emu g (Ni)$^{-1}$] (μ_B f.u.$^{-1}$ Ni)	Calculated Ni content [mol%]	Relative density [%]
0.1	54.2 (0.570)	0.22 (0.0023)	9.8	93
0.2	55.3 (0.581)	0.17 (0.0018)	19.9	93
0.3	55.2 (0.580)	0.06 (0.0006)	29.9	93
0.4	55.5 (0.583)	0.05 (0.0005)	40.0	96
0.5	55.1 (0.579)	0.02 (0.0002)	49.8	92
0.6	55.4 (0.583)	0.04 (0.0004)	60.0	94
0.7	55.3 (0.581)	0.03 (0.0003)	69.9	96
0.8	54.7 (0.575)	0.12 (0.0013)	79.5	96
Pure Ni	55.5 (0.583)	0.22 (0.0024)	100	90
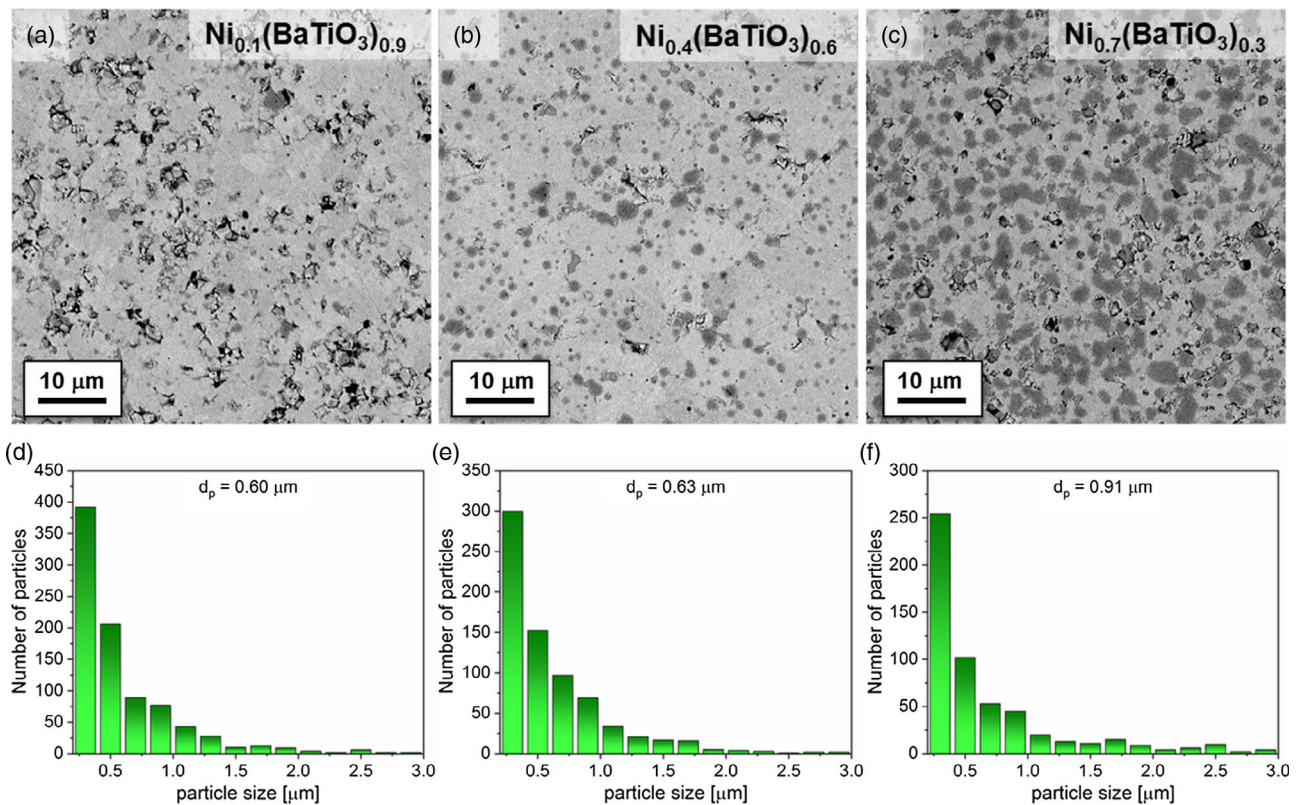
Figure 3. a,b,c) SEM images in BSE mode of polished $Ni_x–(BaTiO_3)_{1-x}$ composites with $x = 0.1$, 0.4, and 0.7. In d,e,f), the corresponding dispersions of grain sizes with the average equivalent spherical diameters d_p are shown.

particles with a larger spread of particle sizes but a similar average value of 0.63 μm. For the 70 mol% Ni sample, larger average nickel particles of 0.91 μm are found. Many of them are not spherical and show a larger degree of agglomeration. In contrast, the percolation limit apparently is not yet reached, as also reflected by the insulating character of the sample. The percolation limit accounts to ≈75 mol% (respectively, 34 vol%).[15,16] For all investigated composites, an intimate and void-free connection of the two components was observed, which clearly is beneficial for magnetoelectric coupling that is widely accepted to be mediated by mechanical deformation, i.e., a combination of the piezoelectric and magnetostrictive properties of two phases.[20]

Supporting EDX analyses were conducted to search for the possible intermixing of the elements, in particular an incorporation of Ni in the $BaTiO_3$ matrix. An EDX linescan is shown in **Figure 4**. The sharp step-wise transitions at the interfaces of two components indicate the absence of significant interdiffusion.

2.2. Magnetic Measurements

Figure 5 shows the field-dependent magnetization curves at 300 K of composites with 10, 40, and 70 mol% Ni in comparison with a pure nickel reference that was manufactured in the same way as the composites. For the composites, the saturation magnetizations have been normalized with respect to the nominal Ni contents. In comparison with the reference, the composites
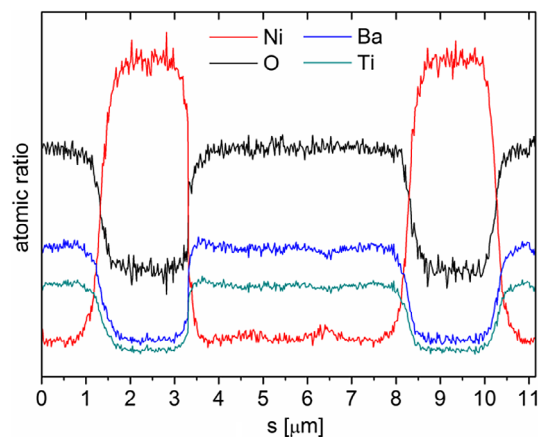
Figure 4. EDX linescan for the $Ni_{0.4}–(BaTiO_3)_{0.6}$ composite.

reach their saturation magnetizations at lower magnetic fields, very likely due to smaller particle sizes. This interpretation is corroborated by an increase in the saturation field with higher x values, which corresponds to their increasing average equivalent particle diameters (from 0.6 [$x = 0.1$] to 0.9 μm [$x = 0.7$]) found in SEM investigations. Another explanation is the possible influence of the $BaTO_3$ matrix on the Ni particles. Cullity and Graham describe a change in the magnetization of polycrystalline nickel caused by tensile and compressive stress. When a
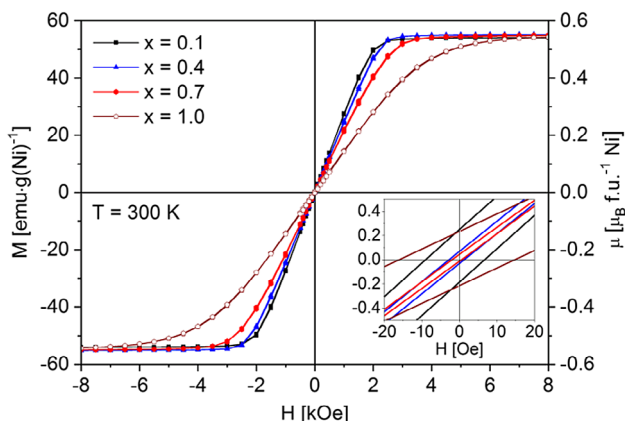
Figure 5. Field-dependent magnetization of selected $Ni_x–(BaTiO_3)_{1-x}$ composites normalized to the nominal Ni content. The low-field region is shown in the inset.

compressive stress is applied, saturation magnetization is reached at a lower magnetic field, and the hysteresis becomes smaller.[21] In our composites, the barium titanate matrix might restrain the magnetostrictive elongation of the nickel particles, leading to compressive stress. With increasing particle size, this effect is expected to decrease in accordance with the experimental findings.

While in Figure 5, only the results for the three selected samples are shown, Table 1 lists the saturation (M_S) and remanent magnetizations (M_R) of all composites. All coercivities are rather small (in the range 1–8 Oe). As the superconducting magnet of the used physical property measurement system (PPMS) may show an intrinsic remanence of up to 20 Oe, these small values

are not significant and are therefore not listed.[22] With the aid of the M_S value of pure nickel, the Ni contents of the composites were calculated. The results listed in Table 1 show deviations below 0.5 mol% with respect to nominal values. This finding proves the correct composition and indicates that a possible formation of mixed phases or a considerable incorporation of Ni in the $BaTiO_3$ matrix can be ruled out. This result is also in accordance with the investigation of Huang et al. who showed that at low oxygen partial pressures nickel is prevented from being integrated in $BaTiO_3$.[14]
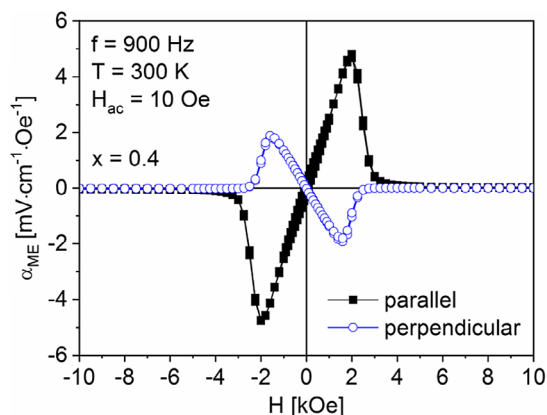
2.3. Magnetoelectric Measurements

The magnetoelectric properties of all composites with nickel contents between 10 and 70 mol% were investigated. The composite with 80 mol% Ni content was conducting and thus not usable. A similar behavior was reported by Tuan and coworkers, who found that the percolation limit was near 34 vol% ($\approx$75 mol%) nickel.[15,16]

In the following paragraphs, only the results for the composite with 40 mol% nickel are shown (Figure 6, 9, and 10) because for the other samples very similar courses were observed. The extracted data for all composites are shown in **Table 2**, and the corresponding plots can be found in Supporting Information.

Figure 6 shows the field dependence of the magnetoelectric coefficient. For both the parallel (∥) and the perpendicular (⊥) sample setups a (centro-) symmetric behavior is found. For $H\|P$, the magnetoelectric coefficient increases linearly between $\approx$−2 kOe and +2 kOe, and after passing a sharp maximum (respectively, minimum at negative field), the magnetoelectric coefficient rapidly decreases to almost zero above $\approx$±4 kOe. Upon reversing the field sweep direction, a small hysteresis

Table 2. Magnetoelectric properties of $Ni_x–(BaTiO_3)_{1-x}$ composites and phase transition temperatures of $BaTiO_3$ in the composites derived from α_{ME} ($t\rightarrow o$ = tetragonal to orthorhombic and $o\rightarrow r$ = orthorhombic to rhombohedral). $H_{C,ME}$ = magnetoelectric coercivity, $H_{max/min}$ = magnetic field of the maximum/minimum of α_{ME}, $\alpha_{ME,max}$ = maximum/minimum values of α_{ME} at H_{max}, and $|\alpha_{ME,\|}/\alpha_{ME,\perp}|$ = ratio of $\alpha_{ME,max}$ in parallel and perpendicular orientations.

| Ni content, x	Orientation	$H_{C,ME}$[Oe]	$H_{max/[min]}$ [Oe]	$\alpha_{ME,max}$ [mV cm^{-1} Oe^{-1}]	$\|\alpha_{ME,\|}/\alpha_{ME,\perp}\|$	$T_{t\rightarrow o}$ [K]	$T_{o\rightarrow r}$ [K]
0						269[10]	177[10]
0.1	∥	155	1800	0.48	2.7	278	192
	⊥	82	1600	−0.18		–	–
0.2	∥	159	1800	1.07	3.3	279	196
	⊥	73	1400	−0.32		297	195
0.3	∥	144	1800	2.04	2.8	277	195
	⊥	41	1400	−0.74		290	198
0.4	∥	94	2000	4.8	2.5	276	196
	⊥	16	1600	−1.93		277	199
0.5	∥	144	1800	2.35	2.2	280	199
	⊥	31	1400	−1.07		288	202
0.6	∥	120	2000	2.95	1.8	277	200
	⊥	2	1200	−1.67		286	205
0.7	∥	180	2250	1.86	1.2	278	202
	⊥	−14	900	−1.59		288	208

Figure 6. Influence of the magnetic DC field on the magnetoelectric coefficient of the $Ni_{0.4}$–$(BaTiO_3)_{0.6}$ sample for parallel (black filled squares) and perpendicular (blue open squares) orientations.

is observed with coercivities ranging from 94 to 180 Oe (Table 2). The direct current (DC) field at which α_{ME} reaches its maximum (H_{max}) is 1800 Oe for $x \leq 0.5$ and increases to 2000 and 2250 Oe for $x = 0.6$ and 0.7, respectively. A comparison of the field-dependent magnetoelectric properties of all samples is given in Figure S3, Supporting Information. The maximum extracted values of the magnetoelectric coefficient (α_{ME}) are shown in **Figure 7**. The values increase with the nickel content up to $4.8 \, mV \, cm^{-1} \, Oe^{-1}$ at $x = 0.4$ and decrease for higher x values. The ratio 40 mol% ferromagnetic/60 mol% ferroelectric component seems to be the generally ideal composition as for this (approximate) ratio, largest α_{ME} coefficients have also been observed for other systems like $CoFe_2O_4$/$BaTiO_3$.[5]

When the magnetic field and polarization are aligned perpendicular, an inverted sign of α_{ME} is observed, i.e., negative values are found at positive magnetic fields, as shown in Figure 6. The DC field at which maximum values of α_{ME} are reached (H_{max}) is significantly lower than in the parallel case and accounts to 1400–1600 Oe for $x \leq 0.5$. H_{max} decreases for larger Ni contents to 1200 and 900 Oe, in contrast with the parallel orientation for which an increase is found. In the region between $\pm H_{max}$, again
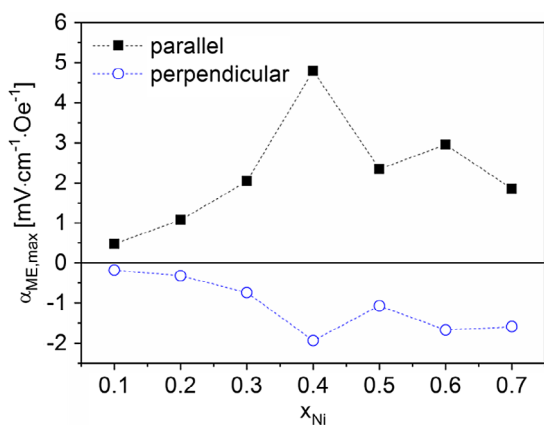
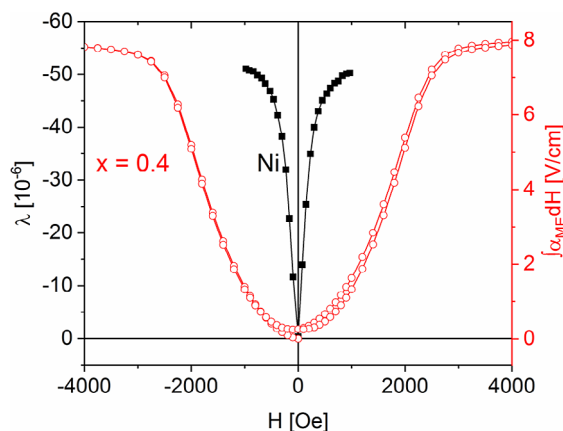a linear behavior is found but the hysteresis is smaller than in the collinear case. The maximum values of $\alpha_{ME,\perp}$ are clearly smaller than in the parallel case but show the same composition trend, as shown in Figure 7. For $x = 0.4$, $\alpha_{ME,\perp}$ reaches $1.93 \, mV \, cm^{-1} \, Oe^{-1}$ which is by a factor of 2.5 smaller than $\alpha_{ME,\|}$. For the other compositions, similar values were observed but the ratio becomes smaller with increasing x.

A similar behavior of ME coupling for parallel and perpendicular orientations (i.e., change in sign and smaller values for $P \perp H$) has also been found for other systems like $(BaTiO_3)_{1-x}$/$(CoFe_2O_4)_x$ with different connectivities (3-3 with $x = 0.38$[8] and 3-0 bulk composites with $x = 0.2$–0.5[23]). For ceramic samples of the system $NiFe_2O_4$-PZT, Zhai et al. systematically measured α_{ME} for angles between H and P from $0°$ up to $90°$. The magnetoelectric coefficient was found to be positive at $0°$ and negative at $90°$ with a factor of 2 for the absolute values. The authors explained this anisotropy by the angle-dependent variation of magnetostriction.[24]

The generally accepted explanation for the origin of the magnetoelectric effect in heterostructures is based on the strain-mediated mechanical coupling between a magnetostrictive and a piezoelectric material.[1,4,20] In turn, the magnetic field dependence of α_{ME} should reflect the magnetostriction. In the applied experimental setup, a small alternating current (AC) field is superimposed to the static magnetic field. As a consequence, α_{ME} is expected to resemble the derivative of the magnetostrictive coefficient λ (i.e., $d\lambda/dH$) or, alternatively, the integration of the α_{ME} coefficient over the magnetic field strength should be proportional to λ, i.e., $\lambda \propto \int \alpha_{ME} dH$.[11,25] In **Figure 8**, data of the magnetostrictive coefficient of nickel taken from Chen et al.[26] are shown together with the integral of α_{ME} for the sample with $x = 0.4$. First, it has to be noted that a negative slope of λ correlates with a positive ME coefficient (please note the different directions of the left and right y-axes in Figure 8). In addition, clear deviations of the two curves are evident. λ shows a peak-like behavior and saturates already around 1000 Oe. In contrast, $\int \alpha_{ME} dH$ has a bell-shaped curve and shows a much higher saturation field of ≈ 3500 Oe. Similarly, these deviations arise from the effect of the additional ferroelectric component. For example, Hrib and Caltun found clear differences in the

Figure 7. Maximum (parallel) and minimum (perpendicular) α_{ME} values of Ni_x–$(BaTiO_3)_{1-x}$ composites (dashed lines are a guide to the eye).


Figure 8. Comparison of the magnetostriction of nickel and the integration of the α_{ME} coefficient of the $Ni_{0.4}$–$(BaTiO_3)_{0.6}$ composite.[25]

magnetostrictive behavior of $CoFe_2O_4$ and $CoFe_2O_4$–$BaTiO_3$ 0-3 heterostructures.[27] Surprisingly, the changes were contrary to the ones we observed, i.e., for the composite, a much sharper, Lorentzian-shaped curve of λ was reported, whereas pure $CoFe_2O_4$ showed a rather broad, Gaussian-shaped behavior. Furthermore, magnetostriction of a given material can be affected by pressure (corresponding to strain due to the surrounding matrix)[28,29] as well as particle size[30]. Such parameters therefore have to be investigated in detail for each composite.

The frequency dependence of α_{ME} is shown in **Figure 9**. Measurements were carried out at 300 K and H_{max} and showed a strong increase up to 400 Hz, and only slightly increasing values up to 1000 Hz without any resonances are obtained. Again, this behavior resembles the one found for $CoFe_2O_4$/$BaTiO_3$.[5,8] Resonances may occur at much higher frequencies that are unfortunately not accessible with our setup.

In **Figure 10**, the temperature dependence of the magnetoelectric coefficient during cooling of the sample with $x = 0.4$ is shown. A clear maximum (for $H \| P$) is observed at a temperature of 276 K, which corresponds to the tetragonal-to-orthorhombic phase transition of $BaTiO_3$. In addition, a step-like
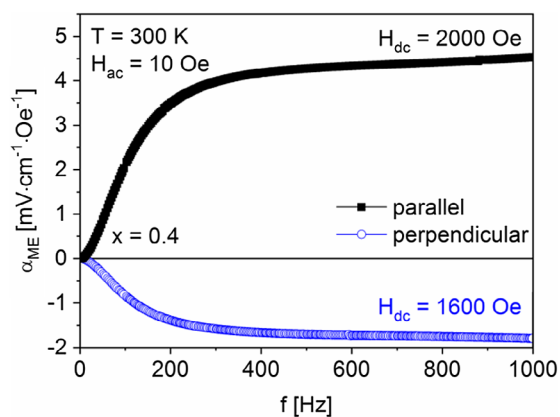
Figure 9. Influence of the frequency of the AC field on α_{ME} for the $Ni_{0.4}$–$(BaTiO_3)_{0.6}$ sample in parallel (black filled squares) and perpendicular (blue open squares) orientation.
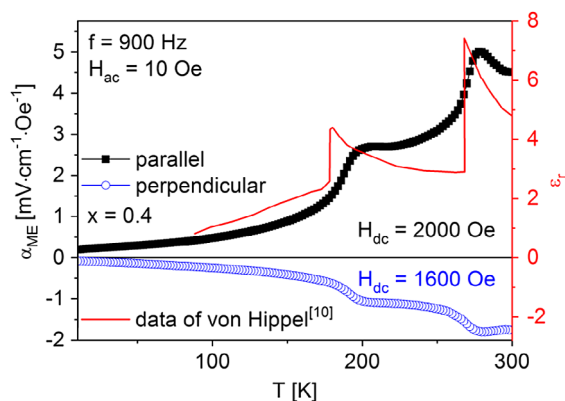
Figure 10. Temperature-dependent magnetoelectric coefficient of the $Ni_{0.4}$–$(BaTiO_3)_{0.6}$ composite in comparison with the dielectric constant (after von Hippel[10]).

decrease in α_{ME} is found at 196 K, which can be assigned to the orthorhombic-to-rhombohedral phase transition temperature. The temperature behavior of α_{ME} (in particular, at the two-phase transitions) resembles the one of the relative permittivity of $BaTiO_3$, as shown for example in the study by von Hippel.[10] As for the other dependencies, $\alpha_{ME,\perp}$ in perpendicular orientation shows the same behavior but with a reversed sign and a smaller magnitude. The transition temperatures of $BaTiO_3$ are known to depend on domain size and substitutions but are generally accepted to be ≈ 273 K ($T_{t \to o}$) and ≈ 183 K ($T_{o \to r}$) during cooling with a significant hysteresis upon heating. The temperature values for our samples derived by a tangent construction are shown in Table 2. For parallel and perpendicular orientations, basically identical values are found, and the differences among the various samples are small and might result from deviating domain sizes. For the $Ni_{0.1}$–$(BaTiO_3)_{0.9}$ sample, the transition temperature for the perpendicular sample orientation could not be determined because of the weak signal.

Our findings are in accordance with the model of strain-mediated mechanical coupling in magnetoelectric composites. In the measured temperature range, the magnetostriction of Ni is basically constant because $T \ll T_C$. Therefore, the mechanical stress applied to $BaTiO_3$ remains similar, and α_{ME} should reflect the temperature dependence of the piezoelectric properties of $BaTiO_3$. As both piezo- and (low-frequency) dielectric properties of $BaTiO_3$ originate from the same ionic displacements (in particular, off-center location of Ti^{4+} within the TiO_6 octahedra), both properties are closely related. In turn, α_{ME} resembles ε_r, as shown in Figure 8. For the different crystallographic modifications of $BaTiO_3$, the di-/piezoelectric properties change because of the different displacements of Ti (along $<111>$ in the rhombohedral, $<110>$ in the orthorhombic, and $<001>$ in the tetragonal modification; for directions given with respect to the cubic system).[10] As a consequence, the structural phase transitions are detectable via the magnetoelectric voltage.

While for other material combinations the effect of phase transition of the ferroelectric component on magnetization has been studied before (e.g., for the combination $BiFeO_3$/$CoFe_2O_4$[31]), to the best of our knowledge, this article and the study by Breitenbach et al.[8] are the only reports on the effect of the low-temperature phase transition of $BaTiO_3$ ($T_{t \to o}$ and $T_{o \to r}$) on the magnetoelectric coefficient. It would also be interesting to study the behavior of α_{ME} at the cubic-to-tetrahedral phase transition but unfortunately, the temperature region above ≈ 350 K is not accessible with our experimental setup.

3. Conclusions

Ni_x–$(BaTiO_3)_{1-x}$ composites ($x = 0.1$–0.8) with 0-3 connectivity have been synthesized, starting from NiO and $BaTiO_3$, by a reducing step in forming gas followed by sintering in nitrogen with graphite as oxygen getter. The resulting samples show densities above 90% and are highly insulating with the exception of $x = 0.8$ for which the percolation limit is reached. According to X-ray powder diffraction, all samples are phase–pure nickel and tetragonal barium titanate. This finding is corroborated

by SEM/EDX investigations, which gave no indications for diffusion of Ni in the $BaTiO_3$ matrix. The SEM investigations showed a good embedding and distribution of basically spherical and isolated nickel particles for small x values. The Ni sizes increase with x, leading to rather agglomerated particles in $Ni_{0.7}$–$(BaTiO_3)_{0.3}$. Magnetic measurements showed a very good agreement of the measured and expected saturation magnetizations corresponding to deviations between the calculated nickel contents and the nominal values below 0.5 mol%.

Detailed magnetoelectric measurements have been carried out and revealed a linear increase in α_{ME} with H until a maximum at $\approx$2000 Oe, whereas for higher fields, the values rapidly decrease. The highest values for the ME coefficients ($\alpha_{ME} = 4.8$ mV cm^{-1} Oe^{-1}) were found for $x = 0.4$ with a collinear orientation of H and P. For $H \perp P$, the magnetoelectric coefficient shows a reversed sign and is roughly by a factor of 2.5 smaller compared with the collinear orientation of P and H. This behavior can be explained by the anisotropy of the magnetostriction.

For all samples, α_{ME} increases strongly with the frequency of the driving AC field up to 400 Hz with only a slight enhancement up to 1000 Hz. The temperature dependence of α_{ME} showed a maximum at $\approx$280 K and a step-like decrease at 195 K. These temperatures correspond to the tetragonal → orthorhombic and the orthorhombic → rhombohedral phase transition of $BaTiO_3$, indicating a strong impact of the crystal structure on the magnetoelectric properties. This finding opens the possibility to conduct structural studies based on temperature-dependent ME measurements and might be a good approach for new sensors. In composites, α_{ME} is generally accepted to be a product property of magnetostriction and piezoelectricity. For our samples, the temperature dependence of α_{ME} closely resembles one of the permittivity of $BaTiO_3$ supporting this model. However, the integral of α_{ME}, which should be proportional to the magnetostriction of the Ni_x–$(BaTiO_3)_{1-x}$ composites, is clearly different from the one of pure nickel. Possible effects of the $BaTiO_3$ matrix on λ of the embedded Ni particles have to be studied further. Thus, the origin of the magnetoelectric coupling in this system remains an interesting research topic.

4. Experimental Section

Material Preparation: Ni_x–$(BaTiO_3)_{1-x}$ composites with $x = 0.1$ up to 0.8 were manufactured. In the first step, $BaTiO_3$ was prepared by a classic mixed oxide synthesis from $BaCO_3$ (Solvay, Sabed VL 600, Lot.-Nr. 538320) and TiO_2 (Venator, TR-HP-2, Lot.-Nr. UOC9410) by calcination at 1373 K for 1 h (heating rate: 5 K min^{-1}) in a Nabertherm box furnace (Type LHT 02/17/P310). The obtained $BaTiO_3$ was milled in a planetary mill PM400 (Retsch) together with stoichiometric quantities of NiO (VEB Berlin-Chemie) with agate balls in an agate jar in isopropanol for 18 h. The mixed powders were pressed at 0.1 MPa into pellets of 6 mm diameter and weights of $\approx$100 mg. Subsequently, NiO was reduced to metallic nickel in a tube furnace (Elite Thermal System Ltd.) at 1073 K in forming gas (Linde, N_2/H_2:90/10; gas flow: 80 mL min^{-1}), applying a heating rate of 5 K min^{-1} and a dwell for 2 h. An oxygen partial pressure of $\approx 5 \times 10^{-24}$ bar was determined using a zirconia sensor (Zirox ZR5) at the furnace outlet. In the final step, the samples were sintered at 1623 K (heating rate: 2.5 K min^{-1}) for 2 h in nitrogen (Linde, 5.0, gas flow: 150 mL min^{-1}) with graphite (Fluka) as the oxygen getter in a horizontal tube furnace HF-1800 (Crystal Systems Corporation). In this step, an oxygen partial pressure of $\approx 10^{-17}$ bar was measured.

Characterization: A Bruker D8-Advance diffractometer (Cu Kα radiation) equipped with a silicon strip LynxEye detector was utilized for room-temperature X-ray powder diffraction investigations (angular range: 15°–70° 2θ, step width = 0.01°, counting time = 0.5 s per data point). Cell parameters of $BaTiO_3$ and Ni of the composites were obtained from Rietveld refinements. The sample surfaces were polished with SiC abrasive paper (grit 2000) and subsequently with 2 μm-diamond suspension using a Struers LaboPol–5. Surface morphology and chemical composition of the sintered samples were investigated by SEM in the backscattered electron mode combined with EDX (acceleration voltage: 15 kV, ZAF-correction method) with a Phenom ProX. With the program ImageJ 1.52a, grain size distributions and average equivalent spherical diameters (d_p) were calculated assuming spherical particles. Magnetic and magnetoelectric investigations were conducted in a Quantum Design PPMS-9. The magnetic measurements were carried out at 300 K in magnetic fields varying between −10 and 10 kOe. Prior to the magnetoelectric measurements, the Ni–$BaTiO_3$ composite pellets with heights between 0.7 and 0.9 mm were sputtered on both sides with 100 nm-thick gold electrodes in a Cressington Sputter Coater 108auto and electrically poled at room temperature, applying a voltage of 800 V for 18 h (Heinzinger LNC 1200–50 pos). Before the magnetoelectric investigations, samples were short circuited for 10 min. The measurements were carried out with the magnetic field parallel and perpendicular to the electrical polarization. A small magnetic AC field (H_{ac}) of 10 Oe was superimposed to the static field by a solenoid and the in-phase voltage (U_{ME}) was recorded using a lock-in technique. Considering the sample thickness d, α_{ME} coefficients were calculated with Equation (1). Details of the set up have been reported in the study by Walther.[32] The magnetoelectric response was analyzed at 300 K as a function of the magnetic DC field for −10 kOe $\leq H_{DC} \leq$ 10 kOe with $f_{(Hac)}$ = 900 Hz. The dependence of α_{ME} on the frequency of the alternating magnetic field was measured from 1 Hz $\leq f_{(Hac)} \leq$ 1000 Hz. Finally, the temperature dependence between 300 and 10 K was measured ($f_{(Hac)}$ = 900 Hz). These measurements were carried out at the DC field of the maximum α_{ME} values.

$$\alpha_{ME} = \frac{U_{ME}}{d \times H_{ac}} \tag{1}$$

Supporting Information

Supporting Information is available from the Wiley Online Library or from the author.

Conflict of Interest

The authors declare no conflict of interest.

[1] M. Fiebig, *J. Phys. D: Appl. Phys.* **2005**, *38*, R123.

[2] N. A. Spaldin, M. Fiebig, *Science* **2005**, *309*, 391.

[3] M. R. Koblischka, *Phys. Unserer Zeit* **2009**, *40*, 132.

[4] J. Ma, J. Hu, Z. Li, C.-W. Nan, *Adv. Mater.* **2011**, *23*, 1062.

[5] T. Walther, U. Straube, R. Köferstein, S. G. Ebbinghaus, *J. Mater. Chem. C* **2016**, *4*, 4792.

[6] M. Breitenbach, S. G. Ebbinghaus, *J. Cryst. Growth* **2018**, *483*, 81.

[7] M. M. Selvi, P. Manimuthu, K. S. Kumar, C. Venkateswaran, *J. Magn. Magn. Mater.* **2014**, *369*, 155.

[8] M. Breitenbach, H. Deniz, S. G. Ebbinghaus, *J. Phys. Chem. Solids* **2019**, *135*, 109076.

[9] R. J. Meyer, E. H. E. Pietsch, *Gmelins Handbuch der Anorganischen Chemie, Titan,* Vol. *41*, 8th edition, Verlag Chemie, Weinheim **1951**, p. 434.

[10] A. von Hippel, *Rev. Mod. Phys.* **1950**, *22*, 221.

[11] H. Palneedi, V. Annapureddy, S. Pirya, J. Ryu, *Actuators* **2016**, *5*, 9.

[12] L. Pauling, *Phys. Rev.* **1938**, *54*, 899.

[13] J. M. Leger, C. Loriers-Susse, B. Vodar, *Phys. Rev. B* **1972**, *6*, 4250.

[14] Y.-C. Huang, S.-S. Chen, W.-H. Tuan, *J. Am. Ceram. Soc.* **2007**, *90*, 1438.

[15] W.-H. Tuan, Y.-C. Huang, *Mater. Chem. Phys.* **2009**, *118*, 187.

[16] W.-H. Tuan, S.-S. Chen, *Ferroelectrics* **2009**, *381*, 167.

[17] H. J. T. Ellingham, *J. Soc. Chem. Ind.* **1944**, *63*, 125.

[18] I. Barin, *Thermochemical Data of Pure Substances*, 3rd edition, VCH, Weinheim **1995**.

[19] G. W. Marks, L. A. Monson, *Ing. Eng. Chem.* **1955**, *47*, 1611.

[20] C. W. Nan, *Phys. Rev. B* **1994**, *50*, 6082.

[21] B. D. Cullity, C. D. Graham, *Introduction to Magnetic Materials*, 2nd edition, Wiley-IEEE Press, Hoboken, NJ **2009**.

[22] Quantum Design, *Application Note 1070–207, Rev. A0*, June **2009**.

[23] S. Agarwal, O. F. Caltun, K. Sreenivas, *Solid State Commun.* **2012**, *152*, 1951.

[24] J. Zhai, N. Cai, Z. Shi, Y. Lin, C.-W. Nan, *J. Phys. D: Appl. Phys.* **2004**, *37*, 823.

[25] Y. Zhou, D. Maurya, Y. Yan, G. Srinivasan, E. Quandt, S. Priya, *Energy Harvest. Syst.* **2016**, *3*, 1.

[26] Y. Chen, B. K. Kriegermeier-Sutton, J. E. Snyder, K. W. Dennis, R. W. McCallum, D. C. Jiles, *J. Magn. Magn. Mater.* **2001**, *1–2*, 131.

[27] L. M. Hrib, O. F. Caltun, *J. Alloys Compd.* **2011**, *509*, 6644.

[28] X. Mu, H.-J. Tang, X.-X. Gao, X.-Q. Bao, J.-H. Li, *Rare Met.* **2015**, https://doi.org/10.1007/s12598-015-0467-8.

[29] G. Altin, K. K. Ho, C. P. Henry, G. P. Carman, *J. Appl. Phys.* **2007**, *101*, 033537.

[30] K. K. Mohaideen, P. A. Joy, *J. Magn. Magn. Mater.* **2013**, *346*, 96.

[31] M. Rafique, A. Herklotz, K. Dörr, S. Manzoor, *Appl. Phys. Lett.* **2017**, *110*, 202902.

[32] T. Walther, *Doctoral Thesis*, Martin-Luther-Universität Halle-Wittenberg, **2018**.